TELKOMNIKA, Vol. 16, No. 5, October 2018, pp.2374~2384
ISSN: 1693-6930, accredited First Grade by Kemenristekdikti, Decree No: 21/E/KPT/2018
DOI:10.12928/TELKOMNIKA.v16i5.9518

SHE Control for PV System Connected to the Grid

Maha Khanfara*, Rachid EL Bachtiri, Oumaima Khanfara, Mohammed Boussetta, Karima EL Hammoumi[5], Imane Idrissi
CED STI, FST, PERE Laboratory EST-USMBA, Fez, Morocco
*Corresponding author, e-mail: maha.khanfara@usmba.ac.ma

Abstract

In this article, we have proposed a new control of a PV system connected to the grid. The goal is to reduce current and voltage harmonicsfor increasing the quality of delivered energy. First, we have modeled a PV panel. Then we have dimensioned the BOOST converter by finding L and C values. Next, we have used Perturb and Observe (P&O) Maximum Power Point Control (MPPT) to improve energy efficiency. Finally, We have developed a control of single-phase H-bridge inverter in order to eliminate the 3^{rd},5^{th},7^{th} and 9^{th} harmonics order, and added an LCLTo connect the PV inverter to the grid, an LCL betweenthe inverter and the grid. Theperformance of the proposed system was tested by computing spectrum and THD usingMatlab/Simulink software. The proposed architecture provides better Total Harmonic Distortion (THD) which satisfy the EN50160 requirement the THD must be less than 4.66%. We found that THD was decreased from 61.93% to 0.04%.

Keywords*: PV array, maximum power point tracking (MPPT), inverter, selective harmonic elimination (SHE)*

1. Introduction

Currently, photovoltaic systems are increased due to adverse environmental effects of conventional energy sources. Photovoltaic installations can be connected to the grid, which represents an important economy in terms of investment and operation. They use the grid as a storage mean. PV system generates power that feeds the grid through one or more converters and transformer. Most of PV systems use rectifiers that operate in inverter mode equipped with a maximum power point tracking.

The power delivered by a photovoltaic panel depend on environmental conditions. To extract the maximum power from a PV panel a maximum power point tracking (MPPT) techniques such as Hill Climbing (HC), Perturb and Observe (P&O), and incremental conductance (IC) are used [1]. PV Module has been presented including maximization of energy production, strategies control to reduce radianceand PV modules orientation. Several researchers present an analysis of the two important MPPT algorithms: the perturb-and-observe (P&O) and incremental conductance (INC). The aim was to clarify the misconceptions prevalent in the literature regarding these two trackers, they have contributed to the performance of the selection process of an appropriate MPPT for researchers and industry [2-4].

In a recent work, P&O and INC have been implemented for a PV inverter, the aim is to prove if INC has a higher performance. Their performance using various perturbation frequencies and amplitudes has been compared. The results suggest that the two algorithms are similar [5]. A three-phase system has been proposed using a PV boost inverter with a mini-boost configuration in order to increase the DC voltage within the influence of radiation to extract the power under the shading [6] and the low levels of radiance, the energy extraction obtained three attenuation design techniques for three phases operating schemes to improve efficiency and common-mode power problems [7].

To obtain a higher yield with a reduction in size [8], weight and cost is the reason that the transformerless inverter is more usable, particularly the electrical network [9], [10]. However, the transformerless inverter suffers from the flow of leakage current through the parasitic capacitors between the PV and the ground. The value of the shedding current depends on the value of the parasitic capacitors the common-mode modulation method of a modified single-phase inverter grid tied flying inductor inverter with MPTT and suppressed leakage current [11].

Received April 6, 2018; Revised August 25, 2018; Accepted September 14, 2018

For cascaded H-bridge inverter there is several configuration and topologies, for the layout of the modular circuit [12], [13]. Various control strategies are proposed in literature to control the converters [14]-[16], including the space vector modulation (SVM), a PV system connected to the grid presents a PWM technic with shifted carrier, the sliding mode control (SMC) and a variable switching frequency (VSF) control technique [17], [18], which control each arm of a dual multilevel inverter [19], and a full wave control to eliminate the first selective harmonics [20]. selective harmonic eliminated pulse width modulation (SHEPWM), is a switching method to achieve minimum harmonic and total harmonic distortion [21], [22].

This paper presents a single phase PV system tied to grid modeling in MATLAB/Simulink. The main contribution is to have a perfect sinusoid for the grid current, thus we applied the P&O based MPPT algorithm to a boost converter in order to elevate the voltage generated by the photovoltaic modules, and a Newton-Raphson method to calculate switching angles in SHE technique, the proposed method was applied for the H-bridge single phase inverter to eliminate the 3rd, 5th, 7th and 9th harmonic. Moreover, a LCL filter has been used to eliminate current and voltage harmonics of the load connected between the inverter and the grid in order to satisfy the grid requirement.

2. System Modeling

2.1. PV Array

The photovoltaic cell used has been described by Equation 1. The equivalent circuit illustrated in Figure 1.

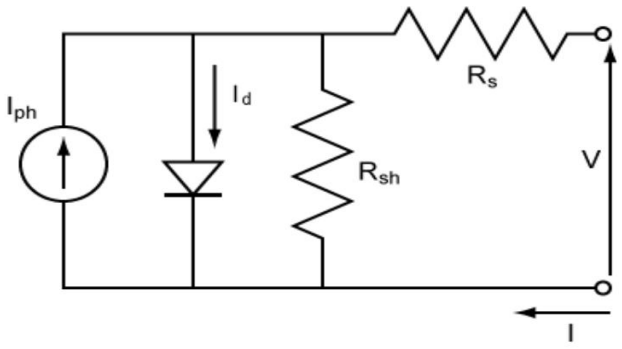

Figure 1. PV equivalent circuit

The characteristic equation of PV cells is given by:

$$I = I_{ph} - I_d - I_p \quad (1)$$

$$I_{ph} = (I_{SC} + K_i \Delta T).\frac{G}{G_{ref}} \quad (2)$$

$$I_d = I_s(\exp\left(\frac{q(V + I.R_s)}{n.KT}\right) - 1) \quad (3)$$

$$I_p = \frac{V_d}{R_p} = \frac{V + I.R_s}{R_p} \quad (4)$$

$$I_s = I_{rs}(\frac{T}{T_{ref}})^3 \exp\{(\frac{1}{T_{ref}} - \frac{1}{T})\}\ \frac{qE_g}{n.K.T} \quad (5)$$

$$I = I_{ph} - I_s\left(\exp\left(\frac{q(V + I.R_s)}{n.KT}\right) - 1\right) - \frac{V + I.R_s}{R_p} \quad (6)$$

The PV array was modeled in SIMULINK using NM55GK panel as shown in Figure 2. The characteristics of the PV Module is given in the Table 1.

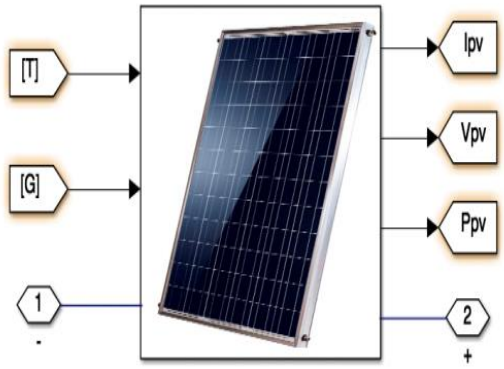

Figure 2. PV array

Table 1. Data sheet of NM55GK PV

Specifications PV module	
Specifications	Value
Open circuit voltage (V_{oc})21.7 *V*	
Short circuit current (I_{sc})3.5 *A*	
Maximum power voltage (V_{mp})17.4 *V*	
Maximum power current (I_{mp})3.16 *A*	
Maximum power rating (P_{mp})55*W*	
Panel Efficiency	12.7%
Fill Factor72.4%	

The I=f(V) and P=f(V) curves of the solar array are illustrated in Figure 3. Simulations were performed at a constant temperature of 25°C at 1000 W/m² irradiation.

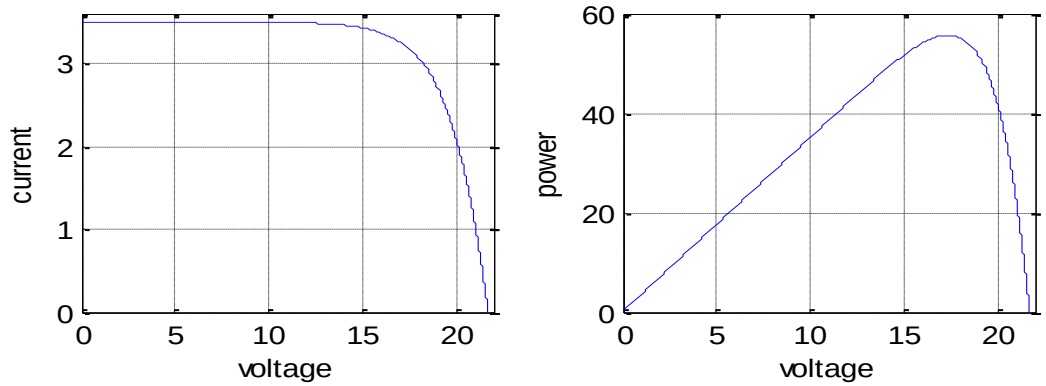

Figure 3. I=f(V) and P=f(V) characteristic of PV panel

2.2. DC-DC Converter

A boost converter has been used. It contains a controlled switch that allows changingthe mean value of a DC voltage source with high efficiency. The structure as shown in Figure 4. requires a controlled switch. The Inductance L smoothest the input current to the source. Capacitor C can limit the output voltage ripple in the circuit diagram when the switch of

the converter is open, the sum of the voltage between L and C gives the boost voltage of the converter. The desired output voltage can be obtained by adjusting the duty cycle of the converter by adopting it with the MPPT control [23].

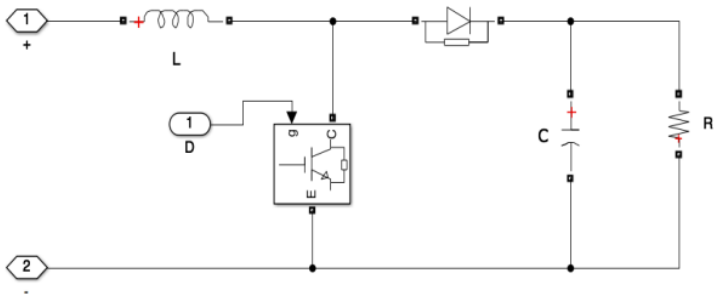

Figure 4. Schematic diagram of boost converter

The booster operation depends on the control of the switch:

a. From 0 to αT: phase of accumulation of energy

The switch is closed (On), the current increase in the inductance thus (storage of magnetic energy). The diode is then blocked and the load is disconnected from the power supply.

b. From αT to T: freewheeling phase

The switch is open; the inductor is then in series with the generator. His fem is added to the generator (booster effect). The current passing through the inductance, the diode D, the capacitor C and the load R. This results in a transfer of the energy accumulated in the inductor to the capacity, which will fix the output voltage. Choice of inductance L: For the first phase (0<t<T)

During the “ON” state

The current is increased when the IGBT is blocked, according to the relation:

$$Ve = L\frac{di}{dt} \qquad i(t) = Im + \frac{Ve}{L}t \tag{7}$$

At the moment t=αT the current in the inductance reaches the peak value:

$$Imax = Imin + \frac{Ve}{L}\alpha T \tag{8}$$

$$Ve - Vs = L\frac{di}{dt} \quad \text{or } Vs - Ve = -L\frac{di}{dt} \tag{9}$$

$$i(t) = Im - \frac{VS - Ve}{L}(t - \alpha T) \tag{10}$$

For the second phase (T <t <T)

$$Ve - Vs = L\frac{di}{dt} \qquad \text{or} \qquad Vs - Ve = -L\frac{di}{dt} \tag{11}$$

At the instant t = T the current in the inductor reaches its minimum value:
Δ_I is the ripple of the current in the inductance

$$\Delta_I = Imax - Imin \tag{12}$$

$$\Delta_{IL}= \frac{Ve}{L}\alpha T \quad (13)$$

At the end of the on state, the I_L current has increased by:

$$\Delta_{IL}= \frac{Ve.\alpha.T}{L} = \frac{V_e.\alpha}{L.F} \quad (14)$$

$$\alpha = 1 - \frac{V_e}{V_s} \quad (15)$$

The inductance dimensioning L, from a given current ripple, is carried out using the following equation:

$$L \geq \frac{V_e.\alpha}{\Delta_{IL}.F} \geq 34MH \quad (16)$$

Choice of capacity C:

To determine the expression of the voltage ripple if it is assumed that the current i_c is perfectly constant. We have the following relation:

$$i_c = c\frac{dv}{dt} \quad (17)$$

For $0 \leq t \leq \alpha t i_s = -i_c$. The resolution of this differential equation gives:

$$Vs = \frac{-i_s}{c}t + V_{Smax} \quad (18)$$

In $t=\alpha t$ we have:

$$Vs\,(t = \alpha t) = V_{Smin} = \frac{-i_s}{c}(\alpha t) + V_{Smax} \quad (19)$$

$$\Delta_{VS}= V_{Smax} - V_{Smin} = \frac{i_s}{c}\alpha t \quad (20)$$

Finally:

$$\Delta_{VS}= \frac{\alpha i_s}{Cf} \quad \text{with} \quad I_s = \frac{V_s}{R} \quad (21)$$

so

$$\Delta_{VS}= \frac{\alpha V_s}{C.f.R} \quad (22)$$

This expression shows us that the voltage ripple decreases when the switching frequency or the value of the capacitor C increase. The dimensioning of the capacitor C from a given voltage ripple is carried out using the following Equation:

$$C \geq \frac{\alpha i_s}{f\Delta_{VS}} \geq \frac{(1-\frac{V_e}{V_s})(1-\alpha)i_e}{f\Delta_{VS}} \geq 450\mu F \quad (23)$$

The MPPT (Maximum Power Point Tracking) command allows extracting the maximum power from the PV generator. The control computes the appropriate duty cycle D. There are several types of MPPT command, in this work we have used the P&O command it consists in

disturbing the Vpv voltage or the Ipv current by a small amplitude around its initial value and analyzing the behavior of the variation of resulting Ppv power. It is widely used because it is easy to implement [24]. The flow chart of P&O algorithm is shown in Figure 5.

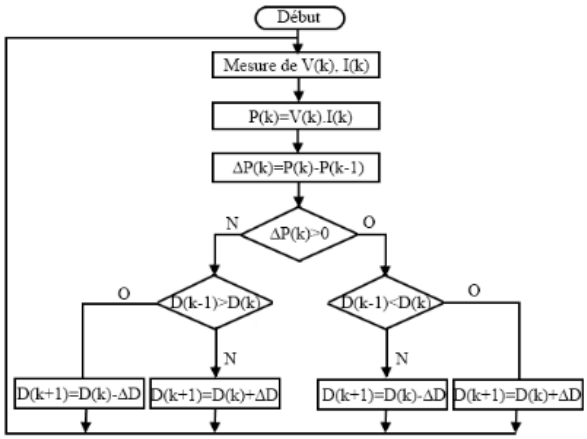

Figure 5. Flowchart of P&O algorithm

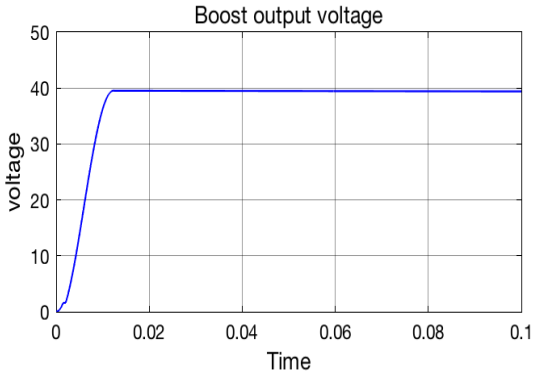

Figure 6. Output voltage of PV boost converter controlled by P&O

2.3. DC-AC Converter

The proposed solution is applied to a cascaded single phase H-bridge inverter shown in Figure 7 and its output voltage in Figure 8. The (SHE) technique in PV inverters problem's is to find an adequate switching angles namely α_1, α_2, α_3 ... α_n so the odd harmonics will be eliminated.

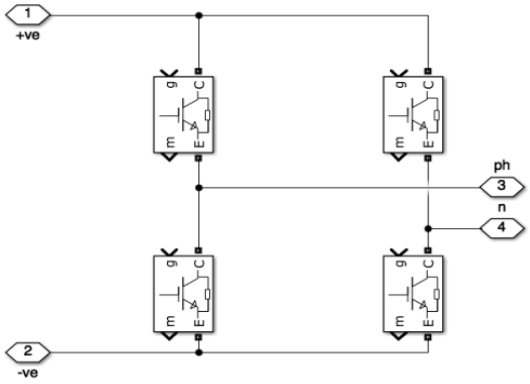

Figure 7. Single phase cascaded H-bridge PV inverter

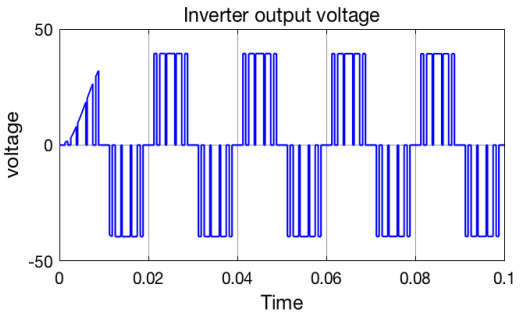

Figure 8. Shows the output voltage of the PV inverter

In our case, the for switching angles (α_1, α_2, α_3 and α_4) must be determined to eliminate the first four odd harmonic components (3rd, 5th, 7th and 9thorder). The solution of the nonlinear equations (24) can be found by applying an iterative technique based on Newton Raphson's method.

$$\begin{aligned} &\cos\alpha_1 + \cos\alpha_2 + \cos\alpha_3 + \cos\alpha_4 + \cos\alpha_5 = m_i\frac{\pi}{4} \\ &\cos 3\alpha_1 + \cos 3\alpha_2 + \cos 3\alpha_3 + \cos 3\alpha_4 + \cos 3\alpha_5 = 0 \\ &\cos 5\alpha_1 + \cos 5\alpha_2 + \cos 5\alpha_3 + \cos 5\alpha_4 + \cos 5\alpha_5 = 0 \end{aligned} \quad (24)$$

$$\cos 7\alpha_1 + \cos 7\alpha_2 + \cos 7\alpha_3 + \cos 7\alpha_4 + \cos 7\alpha_5 = 0$$
$$\cos 9\alpha_1 + \cos 9\alpha_2 + \cos 9\alpha_3 + \cos 9\alpha_4 + \cos 9\alpha_5 = 0$$

Modulation rate m_r is given as follow:
p and A_1 are the number of switching angles and the magnitude of the first harmonic order.

$$m_i = \frac{A_1}{p * E} \tag{25}$$

The resolution of the system (24) is carried out by Newton Raphson method. The five switching angles obtained are shown in Figure 9. The range of the modulation index is m_i= 0:0.01:1.

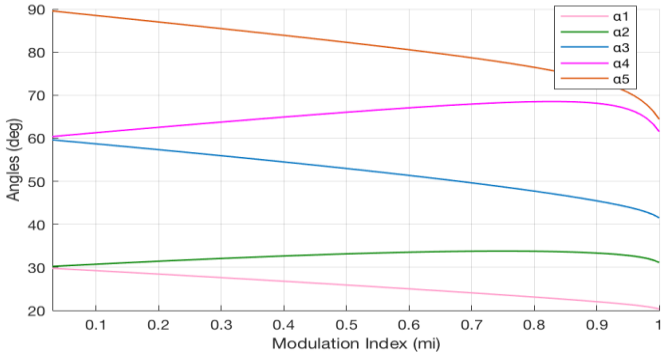

Figure 9. Angles vs Modulation index

The nonlinear equation

$$\begin{aligned} F = [&\cos\alpha_1 - \cos\alpha_2 + \cos\alpha_3 - \cos\alpha_4 + \cos\alpha_5 ; \\ &\cos 3\alpha_1 - \cos 3\alpha_2 + \cos 3\alpha_3 - \cos 3\alpha_4 + \cos 3\alpha_5 : \\ &\cos 5\alpha_1 - \cos 5\alpha_2 + \cos 5\alpha_3 - \cos 5\alpha_4 + \cos 5\alpha_5 ; \\ &\cos 7\alpha_1 - \cos 7\alpha_2 + \cos 7\alpha_3 - \cos 7\alpha_4 + \cos 7\alpha_5 ; \\ &\cos 9\alpha_1 - \cos 9\alpha_2 + \cos 9\alpha_3 - \cos 9\alpha_4 + \cos 9\alpha_5] \end{aligned} \tag{26}$$

And,

$$\begin{aligned} dF = [&-\sin\alpha_1 - \sin\alpha_2 - \sin\alpha_3 - \sin\alpha_4 - \sin\alpha_5 ; \\ &-3\sin 3\alpha_1 - 3\sin 3\alpha_2 - 3\sin 3\alpha_3 - 3\sin 3\alpha_4 - 3\sin 3\alpha_5 ; \\ &-5\sin 5\alpha_1 - 5\sin 5\alpha_2 - 5\sin 5\alpha_3 - 5\sin 5\alpha_4 - 5\sin 5\alpha_5 ; \\ &-7\sin 7\alpha_1 - 7\sin 7\alpha_2 - 7\sin 7\alpha_3 - 7\sin 7\alpha_4 - 7\sin 7\alpha_5 ; \\ &-9\sin 9\alpha_1 - 9\sin 9\alpha_2 - 9\sin 9\alpha_3 - 9\sin 9\alpha_4 - 9\sin 9\alpha_5] \end{aligned} \tag{27}$$

The corresponding harmonic amplitude matrix

$$T = \begin{bmatrix} m_i \frac{\pi}{4} \\ 0 \\ 0 \\ 0 \\ 0 \end{bmatrix} \tag{28}$$

$$d\alpha = \left(INV(dF)\right) * (T - F) \tag{29}$$

Repeat the process for equations (28) and (29), until the switching angles satisfied the desired degree of accuracy, and the solutions must satisfy the condition follow.

$$\alpha_1 < \alpha_2 < \alpha_3 < \alpha_4 < \alpha_5 < \frac{\pi}{2} \quad (30)$$

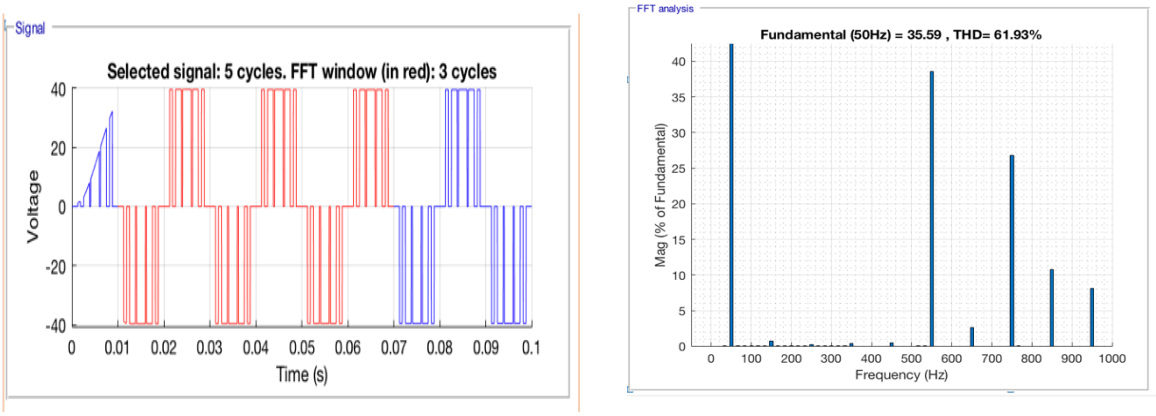

Figure 10. Output voltage of PV inverter and the FFT spectrum of the proposed N-R method.

2.3. LCL Filter

We have used a passive filter LCL to eliminate harmonics above 450 Hz to satisfy the IEEE norm. The line-side inductors of the LCL filter prevent the current harmonics injected from overloading the filter capacitors of the LCL filter.For choosing the LCL filter parameters are calculated in [25]. Figure 11 shows the single-phase LCL filter.

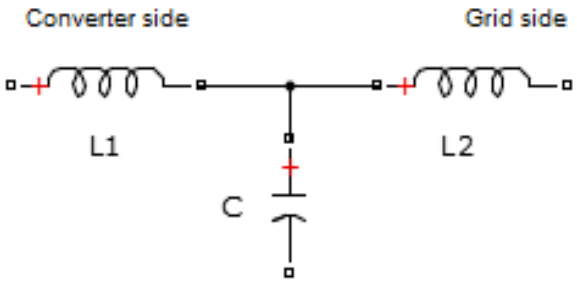

Figure 11. LCL filter single phase

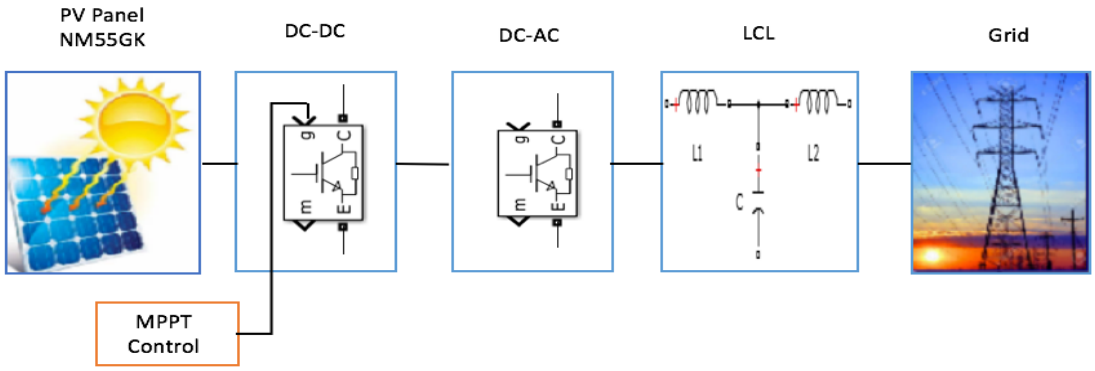

Figure 12. Single phase PV system connected to the Grid

3. Result and Discussion

For low power grid connected applications many research have been proposed. The single phase PV boost inverter system connected to the grid is implemented to supply a resistive load throw a LCL filter as shown in Figure 12. The current output applied on grid side is illustrated in Figure 13, and it's analyzed for the harmonic content and its Fourier spectrum is given in Figure 14. We see that THD was decreased from 61.93% to 0.04% This percentage is within the limits of 4% specified by the IEC. Moreover, the output current and the output voltage are in phase which satisfies the IEEE requirement.

The PV systems must meet stringent power quality requirements set by the utility including low total harmonic distortion (THD) [26] shows the current, voltage and power injected into the grid. For the inverter output voltage, using a LC filter gives a THD about 4 %. The FFT analysis of Selective Harmonic Elimination (SHE) was discussed is reduced from 70.06% to 1.47% by using the LC filter in [27]. A PWM technique appliedto control the inverter It is observed from FFT analysis that the THD of output voltage tied to the grid is about 2.22% [28]. in this work [29]. they used a DC voltage source, a PWM technique to control the inverter and they found that the grid current has a THD of only 0.93%. Compared to those proposed topology of the photovoltaic system in our work we used a Photovoltaic Panel as a voltage source, since the voltage is not stable then we used the P and O method for tracking the maximum power point and a SHE technique to control the inverter.

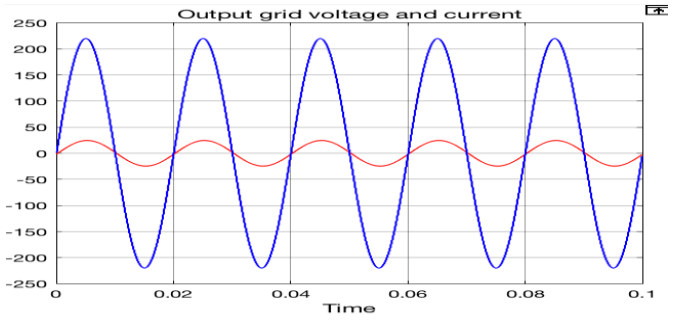

Figure 13. Output grid voltage and current

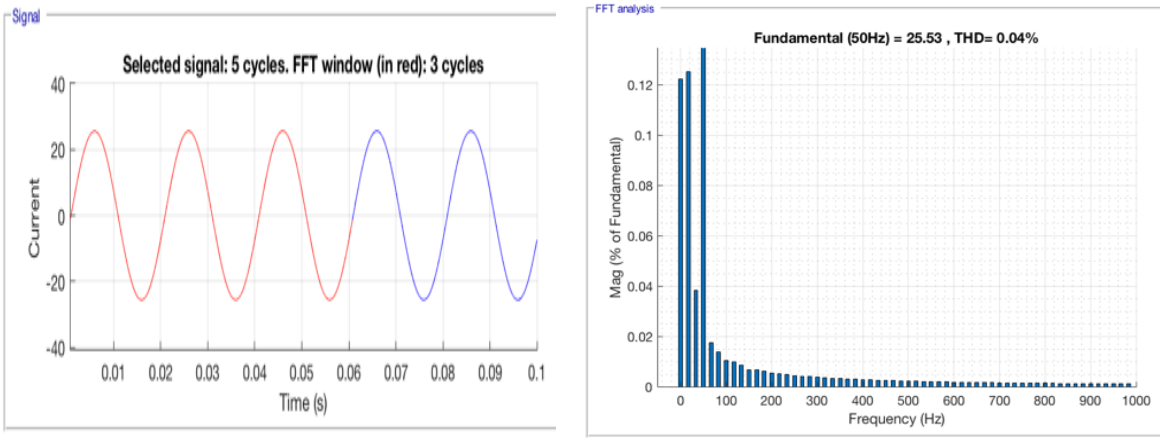

Figure 14. Output grid current and the FFT spectrum

4. Conclusion

In this paper, a new architecture of PV grid-connected H-bridge cascaded single phase inverter was studied. A proposed MPPT algorithm is implemented to improve energy conversion efficiency and a boost converter sizing was achieved. A SHE technique using Newton Raphson

method to find out the switching angles for an adequate PWM control the objectives are achieved by eliminating the first four odd harmonics of the output inverter voltage. The main contribution of this work is to reduce current and voltage load harmonics and increase the quality of delivered energy by the PV system tied to the grid through a low-pass filter. We have used an LCL filter to provide better harmonic attenuation. The THD was decreased from 61.93% to 0.04% which satisfy the IEEE requirement.

References

[1] MA Ghasemi, A Ramyar, H Iman-Eini. MPPT Method for PV Systems under Partially Shaded Conditions by Approximating I-V Curve. *IEEE Trans. Ind. Electron*. 2018; 65(5): 3966–3975.

[2] D Sera, R Teodorescu, J Hantschel, M Knoll. *Optimized Maximum Power Point Tracker for fast changing environmental conditions*. IEEE Int. Symp. Ind. Electron. 2008: 2401–2407.

[3] MAG De Brito, L Galotto, LP Sampaio, G De Azevedo Melo, CA Canesin. Evaluation of the main MPPT techniques for photovoltaic applications. *IEEE Trans. Ind. Electron*. 2013; 60(3): 1156–1167.

[4] D Sera, L Mathe, T Kerekes, SV Spataru, R Teodorescu. On the perturb-and-observe and incremental conductance mppt methods for PV systems. *IEEE J. Photovoltaics.* 2013; 3(3): 1070–1078.

[5] SB Kjær. Evaluation of the hill climbing and the incremental conductance maximum power point trackers for photovoltaic power systems. *IEEE Trans. Energy Convers*. 2012; 27(4): 922–929.

[6] S Motahhir, A El Ghzizal, A Derouich. Shading Effect to Energy Withdrawn from the Photovoltaic Panel and Implementation of DMPPT Using C Language Shading effect to energy withdrawn from the photovoltaic panel and implementation of DMPPT using C language Abbreviations. 2017: 2016.

[7] D Sera, L Mathe, T Kerekes, SV Spataru, R Teodorescu. On the perturb-and-observe and incremental conductance mppt methods for PV systems. *IEEE J. Photovoltaics.* 2013; 3(3): 1070–1078.

[8] M Khanfara, R El Bachtiri, M Boussetta, K El Hammoumi. *Economic Sizing of a Grid-Connected Photovoltaic System :Case of GISER research project in Morocco*. IOP Conference Series : Earth and Environmental Science. 2018; 161(1): 012006.

[9] JF Ardashir, M Sabahi, SH Hosseini, F Blaabjerg, E Babaei, GB Gharehpetian. A Single-Phase Transformerless Inverter with Charge Pump Circuit Concept for Grid-Tied PV Applications. *IEEE Trans. Ind. Electron*. 2017; 64(7): 5403–5415.

[10] SR Aghdam, E Babaei, S Laali. *Maximum constant boost control method for switched-inductor Z-source inverter by using battery*. IECON Proc. (Industrial Electron. Conf. 2013: 984–989.

[11] M Tofigh Azary, M Sabahi, E Babaei, F Abbasi Aghdam Meinagh. Modified Single-Phase Single-Stage Grid-Tied Flying Inductor Inverter With MPPT and Suppressed Leakage Current. *IEEE Trans. Ind. Electron*. 2018; 65(1): 221–231.

[12] NNVS Babu, BG Fernandes. *Cascaded Two-Level Inverter-Based Multilevel STATCOM for High-Power Applications*. IEEE Transactions on Power Delivery. June 2014; 29(3): 993-1001.

[13] M Khanfara, R El Bachtiri, K El Hammoumi, M Boussetta. *A comparison between two filters for PV inverter controlled to eliminate firsts harmonics*. 2016 Int. Conf. Inf. Technol. Organ. Dev. IT4OD 2016. 2016: 9–14.

[14] S Kouro et al. Recent Advances and Industrial Applications of Multilevel Converters. *IEEE Trans. Ind. Electron*. 2010; 57(8): 2553–2580.

[15] A Jidin, T Sutikno. Matlab/Simulink Based Analysis of Voltage Source Inverter with Space Vector. 2009; 7(1): 23–30.

[16] R Palanisamy, K Vijayakumar. Paper SVPWM for 3-phase 3-level neutral point clamped inverter fed induction motor control. *Indonesian Journal of Electrical Engineering and Computer Science (IJEECS)*. 2018; 9(3): 703–710.

[17] M Malinowski, K Gopakumar, J Rodriguez, MA Perez. A survey on cascaded multilevel inverters. *IEEE Trans. Ind. Electron*. 2010; 57(7): 2197–2206.

[18] N Kumar, TK Saha, J Dey. Sliding-Mode Control of PWM Dual Inverter-Based Grid-Connected PV System: Modeling and Performance Analysis. *IEEE J. Emerg. Sel. Top. Power Electron*. 2016; 4(2): 435–444.

[19] N Kumar, TK Saha, J Dey. Sliding-Mode Control of PWM Dual Inverter-Based Grid-Connected PV System: Modeling and Performance Analysis. *IEEE J. Emerg. Sel. Top. Power Electron*. 2016; 4(2): 435–444.

[20] M Khanfara, R El Bachtiri, K El Hammoumi, M Boussetta. *A comparison between two filters for PV inverter controlled to eliminate firsts harmonics*. 2016 Int. Conf. Inf. Technol. Organ. Dev. IT4OD 2016. 2016: 9–14.

[21] N Kumar, TK Saha, J Dey. Sliding-Mode Control of PWM Dual Inverter-Based Grid-Connected PV System: Modeling and Performance Analysis. *IEEE J. Emerg. Sel. Top. Power Electron*. 2016; 4(2): 435–444.

[22] MS Patil, SD Patil, PP Debre. Comparison of PWM Techniques and Selective Harmonic Elimination for 3-Level Inverter. *International Journal of Engineering Research and Applications.* 2016; 6(4): 16-20.
[23] S Motahhir, A El Ghzizal, S Sebti, A Derouich. MIL and SIL and PIL tests for MPPT algorithm. *Cogent Eng*. 2017; 4(1).
[24] S Motahhir, A El Ghzizal, S Sebti, A Derouich. *Proposal and implementation of a novel perturb and observe algorithm using embedded software*. Proc. 2015 IEEE Int. Renew. Sustain. Energy Conf. IRSEC 2015. 2016.
[25] M Liserre, F Blaabjerg, S Hansen. *Design and control of an LCL-filter based three-phase active rectifier*. Conf. Rec. 2001 IEEE Ind. Appl. Conf. 36th IAS Annu. Meet. (Cat. No.01CH37248). 2005; 1(5): 299–307.
[26] BA Allah, L Djamel. Control of Power and Voltage of Solar Grid Connected. *Bulletin of Electrical Engineering and Informatics (BEEI)*. 2016; 5(1): 1–8.
[27] V Karthikeyan, VJ Vijayalakshmi, P Jeyakumar. Selective Harmonic Elimination (SHE) for 3-Phase Voltage Source Inverter (VSI). *Am. J. Electr. Electron. Eng*. 2014; 2(1): 17–20.
[28] M Satyanarayana, P Satish Kumar. Analysis and Design of Solar Photo Voltaic Grid Connected Inverter. *Indonesian Journal of Electrical Engineering and Informatics (IJEEI)*. 2015; 3(4): 199–208.
[29] B Bolsens, K De Brabandere, J Van Den Keybus, J Driesen, R Belmans. *Model-based generation of low distortion currents in grid-coupled PWM-inverters using an LCL output filter*. PESC Rec.-IEEE Annu. Power Electron. Spec. Conf. 2004; 6(4): 4616–4622.